Simple model for competitive dynamics among dendritic sidebranches

Hidetsugu Sakaguchi, Kazuki Kishinawa, Kyohei Katsuki, and Haruo Honjo
Department of Applied Science for Electronics and Materials, Interdisciplinary Graduate School of Engineering Sciences, Kyushu University, Kasuga, Fukuoka 816-8580, Japan
(Received 8 November 2006; published 23 February 2007)

We study competitive dynamics among sidebranches in the crystal growth of dendrites. Numerical simulations are performed with a coupled map lattice to investigate the competitive dynamics among dendritic branches. A simple form of interaction via a diffusion field is estimated from the numerical simulations of the coupled map lattice. We propose a needle model on the basis of the competitive interaction, and perform numerical simulations of it. The size distribution of the dendritic branches exhibits a power law in the needle model.

DOI: 10.1103/PhysRevE.75.021606 PACS number(s): 81.10.Aj, 05.45.Ra, 05.45.Df

I. INTRODUCTION

The dendrite is a typical pattern in crystal growth. The tip velocity and the parabolic shape near the tip region have been intensively studied [1,2]. Many sidebranches appear far from the dendritic tip in experiments on succinonitrile and NH_4Cl. Huang and Glicksman investigated the development of sidebranches in an experiment on succinonitrile [3]. The sidebranches compete with each other. Active sidebranches grow faster and suppress the shorter sidebranches. The growth velocity of the shorter branches becomes slower and slower, and the shorter ones finally stop growing, because the diffusion field is screened off by the active branches. The envelope shapes formed by the active sidebranches and the spacing between the sidebranches have been experimentally investigated by several authors [4–6]. Li and Beckermann studied a nonlinear coarsening process by the competition among the sidebranches [5]. Recently, Couder *et al.* studied the competitive time evolution of the sidebranches including the shorter sidebranches. They found that the length of inactive shorter sidebranches saturates in time in an exponential manner [7]. In this paper, we will investigate the competitive dynamics of the sidebranches, in particular, the dynamics of the inactive shorter sidebranches.

On the other hand, scale invariance characterized by a power law is often observed in several growth models such as diffusion-limited aggregation (DLA). Several types of needle models have been proposed to study the competitive dynamics among branches more explicitly [8–10]. In two dimensions, needles grow only in the upward direction without the tip splitting, starting from a basal line. Needles interact with neighboring needles, and some grow faster, which suppress the growth of shorter needles. Such needle models are useful for the understanding of the competitive dynamics among the sidebranches of dendrites. Further, these models are suggestive for more general competitive systems such as trees in a forest and ecological and social systems [11,12].

In this paper, we first study the competitive dynamics among dendritic sidebranches using a coupled map lattice and then propose a different needle model. The needle model can be solved explicitly, and the size distribution of sidebranches exhibits a power law in the needle model.

II. COMPETITIVE GROWTH OF SIDEBRANCHES IN A COUPLED MAP LATTICE MODEL

Phase-field models have been commonly used for the numerical simulation of dendrites [13–15]. The sidebranching was also studied using the phase-field models [16,17]. However, a large-scale numerical simulation of the phase-field model is rather time consuming under the condition of small supercooling, because the phase-field models are coupled partial differential equations. We have proposed a coupled map lattice model as a simple simulation method for crystal growth, and succeeded in reproducing various patterns such as DLA and dendrites [18]. Compared with the phase-field model, the coupled map lattice is a simple model and it is very efficient for a large-scale numerical simulation even at small supercooling. It was shown that the law $v\rho^2=$const, where ρ is the radius of curvature near the tip of the dendrite and v is the tip velocity, is approximately satisfied at small supercooling in the coupled map lattice [19]. The envelope and the spacing between the active sidebranches were also numerically studied with the coupled map lattice model [20]. Power law growth of the sidebranches is observed when the spacing between the neighboring sidebranches is small, and the concentration field around the sidebranches was also studied [20]. The coupled map lattice was further applied to the oscillatory growth in electrodeposition of Sn [21].

In the coupled map lattice model, there are two variables; one variable u denotes a diffusion field such as concentration in the solution growth, and the other variable x is an order parameter which indicates the degree of crystallization at each lattice point. The order parameter x takes a continuous value between 0 and 1 at interface sites. Time evolutions are performed in two steps on each lattice point. The fourfold rotational symmetry of the crystal is involved in performing the simulation on a square lattice. The first step is a diffusion process and the second step is a growth process at the interface. The diffusion process on a square lattice is expressed as

$$u_t'(i,j) = u_t(i,j) + D\Delta t/\Delta x^2\{u_t(i+1,j) + u_t(i-1,j) + u_t(i,j+1) + u_t(i,j-1) - 4u_t(i,j)\}, \quad (1)$$

where u and u' denote dimensionless concentrations, t is an integer step number, Δt is a time step, (i,j) is a coordinate of the lattice point, and D is the diffusion constant. This process is interpreted as the simplest difference equation corresponding to the diffusion equation $\partial u/\partial t = D\nabla^2 u$. The second step is a growth process at the interface. The order parameter $x(i,j)$ is set to be 0 in the solution sites and 1 in the crystal sites. The order parameter $x(i,j)$ changes only at the interface sites. The growth rule of x and u at the interface sites is written as

$$x_{t+1}(i,j) = x_t(i,j) + \gamma\Delta t u_t'(i,j),$$

$$u_{t+1}(i,j) = u_t'(i,j) - \gamma\Delta t u_t'(i,j), \quad (2)$$

where γ denotes the incorporation rate of the solute into the crystal at the interface sites. In this paper, we have assumed that $D=0.2$, $\Delta t=1$, $\Delta x=1$, and $\gamma=1$ for the sake of simplicity. If $x(i,j)$ goes over the threshold 1, the lattice site is interpreted as being crystallized, and the interface moves by one site. The initial concentration is assumed to be uniform $u(i,j)=u_0$ in regions other than areas where a seed of crystal exists. The parameter u_0 represents supersaturation in our model.

We have performed a numerical simulation for $u_0=0.1$. The system size is 500×500. Periodic boundary conditions are used as the lateral boundary conditions. A seed of a crystal is set on a line $y=1$ as an initial condition. Many dendrites grow from the linear seed. The initial value of x at the linear interface site is distributed randomly between 0 and 0.1. Figure 1(a) displays a snapshot pattern of many dendritic branches. Various sizes of dendritic branches appear. Taller branches are active and suppress the growth of the shorter branches. Small horizontal sidebranches appear from each vertical dendrite. The growth of the small horizontal sidebranches is more active for the taller branches, in particular, at the side where there is wider open space. Figure 1(b) displays time evolutions of four dendritic tips at $i=158$, 171, 187, and 315. The growth velocities of the shorter branches other than $i=171$ decrease in time and become zero. The height of each short branch approaches a constant value exponentially in time, although the final height and the decay constant are different for different branches. The decay constant for a shorter branch is generally larger than that for a taller branch. Figure 1(c) displays a double-logarithmic plot of the height distribution of dendritic branches at the final simulation time $t=400\,000$ for $u_0=0.1$, which is obtained using 50 ensembles with different random initial conditions. Although several tallest branches are still growing, most branches, whose heights are shorter than about 200, stop growing. The height distribution $P(y)$ is approximated by a power law $l^{-\alpha}$ with $\alpha\sim1.9$ for $y>5$.

III. DIFFUSION FIELD AROUND STEADILY GROWING DENDRITES

The competition among many dendritic branches arises through the concentration field. It is rather difficult to solve the diffusion field with the moving interface. If dendritic branches with growth velocity v are periodically arranged at a constant interval of L, and the shape of each dendrite is approximated by a rectangle as shown in Fig. 2(a), the diffusion field can be solved approximately by assuming $u(x,y,t)=u(x,y-vt)$. Then, the diffusion equation is expressed as

$$-v\frac{\partial u}{\partial y} = D\left(\frac{\partial^2 u}{\partial x^2} + \frac{\partial^2 u}{\partial y^2}\right), \quad (3)$$

where $y-vt$ is rewritten as y, and the tip position of the dendritic branches is assumed to be $y=0$. The boundary conditions are $u(x,\infty)=u_0$ and $u(x,-\infty)=0$. The other boundary condition is $u(x,y)=0$ inside the dendritic branches, which are located at $nL-Lu_0/2<x<nL+Lu_0/2$ and $y<0$. Here, n is an integer and the width of the dedritic branches is assumed to be u_0L owing to the conditions of steady growth and the conservation law of u. The solution of this equation, satisfying the boundary conditions and the mirror symmetry around $x=0$, is expressed by a Fourier series expansion as

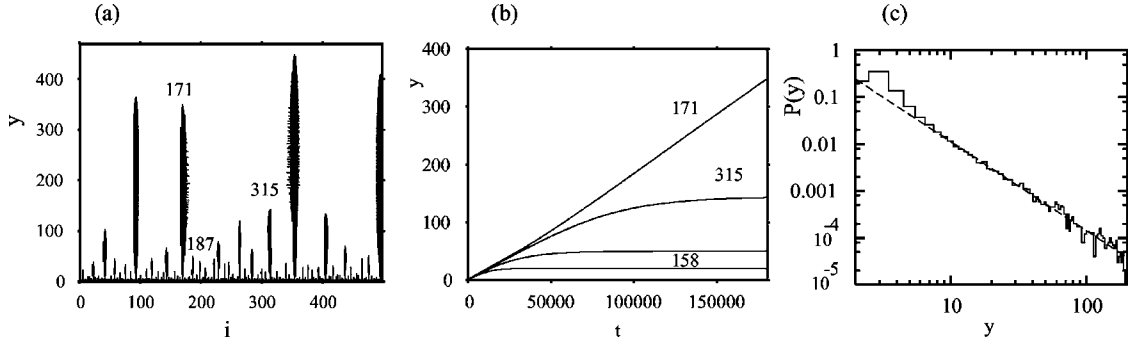

FIG. 1. (a) Snapshot of dendritic pattern for $u_0=0.1$ in a coupled map lattice model. (b) Time evolutions of tip positions of four dendritic branches at $i=158$, 171, 187, and 315. The taller three dendrites at $i=171$, 315, and 187 are indicated in (a). (c) Height distribution of dendritic branches. The dashed line is $P(y)\sim y^{-1.9}$ for $y<200$.

$$u(x,y) = \begin{cases} u_0(1 - b_0 e^{-k_0' y}) + \sum_{n=1}^{N} b_n \cos(2\pi n x/L) e^{-k_n' y} & \text{for } y > 0, \\ \sum_{n=1}^{N} a_n \sin\{\pi(2n-1)(x - Lu_0/2)/L(1-u_0)\} e^{k_n y} & \text{for } y < 0, \end{cases} \tag{4}$$

where $k_n' = 1/2[v/D + \sqrt{(v/D)^2 + 4(2\pi n/L)^2}]$ and $k_n = 1/2 \times [-v/D + \sqrt{(v/D)^2 + 4\{\pi(2n-1)/L(1-u_0)\}^2}]$. Note that $1/k_0' = D/v$ is a diffusion length, and $k_n' > 0, k_n > 0$. The Fourier amplitudes b_n and a_n are determined by the continuity conditions of u and $\partial u/\partial y$ at $y=0$, which are expressed as

$$u_0(1 - b_0) = \sum_{n=1}^{N} 2a_n \frac{1 - u_0}{\pi(2n-1)},$$

$$b_m/2 = \sum_{n=1}^{N} \frac{a_n \cos(m\pi u_0)(1-u_0)}{\pi} \left(\frac{1}{2m(1-u_0) + (2n-1)} - \frac{1}{2m(1-u_0) - (2n-1)} \right), \quad m = 1,2,\ldots,N,$$

$$u_0 b_0 k_0' + \sum_{m=1}^{N} b_m \cos\left(\frac{2\pi m}{L} \{u_0 L/2 + L(1-u_0) j/(2N)\} \right)(-k_m') = \sum_{n=1}^{N} a_n \sin\{(2n-1)\pi j/(2N)\} k_n, \quad j = 1,2,\ldots,N. \tag{5}$$

The Fourier amplitudes a_n and b_n are solutions to the coupled linear equations (5).

The concentration $u(x,y)$ at the middle line $x=L/2$ between the neighboring two branches is expressed as

$$u(L/2,y) = \sum_{n=1}^{N} a_n (-1)^{n-1} e^{k_n y} \quad \text{for } y < 0. \tag{6}$$

If $|y|$ is large, $u(L/2,y)$ is approximated only by the first term as

$$u(L/2,y) = a_1 e^{k_1 y}. \tag{7}$$

Figure 2(b) compares the concentration field $u(x,y)$ (solid curve) at the middle line in the coupled map lattice model for $u_0=0.15$ and $L=80$ with the concentration $u(L/2,y)$ (dashed curve) obtained from Eq. (6) for $L=80$, $u_0=0.15$, $N=10$, and $v=0.0104$. Here, the tip velocity $v=0.0104$ is the one obtained by the numerical simulation of the coupled map lattice. Figure 2(c) compares the concentration u by Eq. (6) with the approximation of u by Eq. (7) with $a_1=0.0102$ and $k_1=0.026\,54$. The good agreement shows that the approximation of the concentration field u by a single exponential function is rather good.

IV. COMPETITIVE GROWTH AMONG A FEW DENDRITES

Competitive dynamics among many dendrites is rather difficult. We first investigate competitive dynamics between two dendrites. We consider a periodic array of dendrites with intervals of $L/2$ as shown in Fig. 2(a), and the heights of the two dendritic branches are different as an initial condition. The taller dendrite grows faster and the velocity of the shorter one decreases in time. Figure 3(a) is a snapshot of the two dendrites at $u_0=0.1$ and $L=100$. Periodic boundary conditions are used as the lateral boundary conditions. The tip positions of the taller and shorter dendrites are expressed as (i_1,y_1) and (i_2,y_2). Here, the tip position is defined for example as $y_2 = j_{2,max} + x(i_2, j_{2,max}+1)$, where $j_{2,max}$ is the maximum crystallized site on the line $i=i_2$, because $x(i_2, j_{2,max}+1)$ represents the degree of crystallization at the interface site $(i_2, j_{2,max}+1)$. Figure 3(b) displays a semilogarithmic

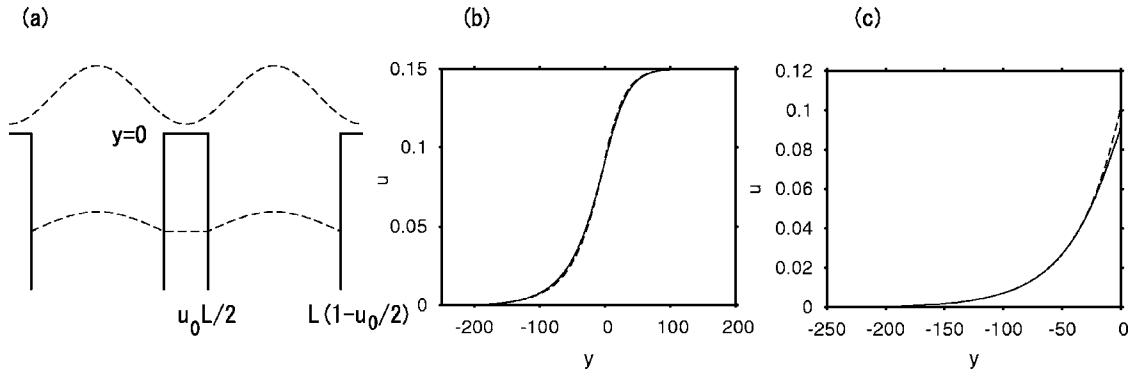

FIG. 2. (a) Configuration of a periodic array of dendrites and schematic plots (dashed curves) of $u(x,y)$ for $y>0$ and $y<0$. (b) Concentration field $u(x,y)$ at $x=L/2$ by the coupled map lattice model (solid curve) and by Eq. (6) (dashed curve) at $u_0=0.15$ and $L=80$. (c) Comparison of Eq. (6) (solid curve) and Eq. (7) (dashed curve).

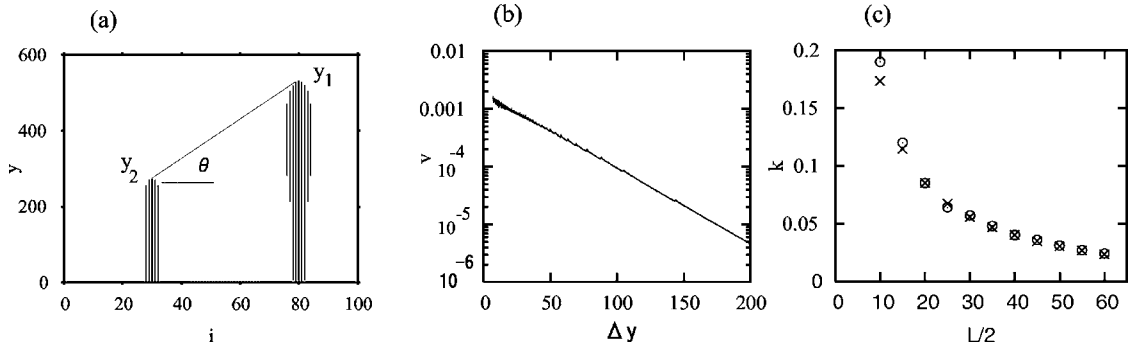

FIG. 3. (a) Snapshot growth pattern of two dendrites for $u_0=0.1$ and $L=100$. (b) Semilogarithmic plot of the growth velocity of the shorter dendrite as a function of the size difference Δy of the two dendrites. (c) Comparison of the decay rate k (circle) in the coupled map lattice model and $k_1(L)$ (cross) for the diffusion field.

plot of the growth velocity dy_2/dt of the shorter dendrite as a function of the height difference $\Delta y=y_1-y_2$. The growth velocity of the shorter dendrite decays approximately as $dy_2/dt \sim \exp(-k\Delta y)$. The decay constant k is 0.031. Figure 3(c) displays the relation of the decay constant k (circle) as a function of the interval $L/2$ between the two dendrites. The crosses denote the decay rate $k_1(L)=1/2[-v/D+\sqrt{(v/D)^2+4\pi^2/\{L(1-u_0)\}^2}]$ calculated in the previous section, where v is evaluated as the tip velocity of the taller dendrite. The decay rate k of the growth velocity of the shorter dendrite was evaluated when the shorter dendrite is strongly screened off by the taller dendrite. It is natural that the decay rate k of the growth velocity of the shorter dendrite is close to another decay rate $k_1(L)$ of the concentration field u on the middle line $x=L/2$ between the taller dendrites. That is, the growth velocity of the shorter dendrite is approximately expressed as $dy_2/dt=dy_1/dt \exp\{-k_1(L)(y_1-y_2)\}$. Here, we have made use of the fact that the velocities of the two dendrites are the same, if the heights of the two dendrites are the same, i.e., $y_1=y_2$. If v/D is sufficiently smaller than $2\pi/L$, $k_1(L)\sim\pi/\{L(1-u_0)\}$. Then, $dy_2/dt \sim dy_1/dt \exp[-\pi/\{L(1-u_0)\}(y_1-y_2)]=dy_1/dt \exp[-\pi/\{2(1-u_0)\}\tan\theta]$, where θ is a screening angle satisfying $\tan\theta=(y_1-y_2)/(L/2)$ as shown in Fig. 3(a). The screening effect by the taller dendrites was analyzed using the screening angle by Couder *et al.* [7]. Our result supports their analysis, when v/D is very small. However, the exponential term is approximated as $\exp[-(D/v)\pi^2/\{L^2(1-u_0)^2\}(y_1-y_2)]=\exp[-(D/v)\pi/\{2L(1-u_0)^2\}\tan\theta]$ and the analysis using only $\tan\theta$ is not good, when $2\pi/L$ is sufficiently smaller than v/D.

If the shorter dendrite is not located exactly on the middle line between the two taller dendrites but located at $i_2=i_1-\Delta x$, the growth velocity of the shorter dendrite will become even smaller, because the concentration field u there is smaller than that is on the middle line. The concentration field u is roughly expected to be

$$u(i_2,y) \sim a_1 e^{k_1 y} \sin(\pi\Delta x/L). \tag{8}$$

Here, we have neglected the effect of nonzero u_0, because the thickness of the dendrites changes when one dendrite overcomes the other, and the width of the dendrite is small near the dendritic tip. Figure 4(a) displays a snapshot pattern of two dendrites at $i_2=30$ and $i_1=50$. Owing to the periodic boundary conditions, a small dendrite with height y_2 and a large dendrite with height y_1 are assumed to exist respectively at $i=130$ and -50, although they are not shown in Fig. 4(a). The initial position of the taller dendrite is changed as $i_1=40,50,\ldots,80$, and we have thus calculated the growth velocity v_1 of the shorter dendrite. The growth velocity v_1 becomes smaller as Δx is smaller. The growth velocity for $\Delta x=L/2$ is denoted as v_{10}. Figure 4(b) displays the ratio v_1/v_{10} (plus), when the height difference is $\Delta y=150$. The dashed line represents $\sin(\pi\Delta x/L)$. Thus, we have found that the time evolution of the shorter dendrite can be approximated by

$$dy_2/dt \sim (dy_1/dt)\exp[-k_1(L)(y_1-y_2)]\sin(\pi\Delta x/L).$$

Next, we consider the competitive dynamics among four dendrites, which are located at $i=0$, $L/4$, $2L/4$, and $3L/4$, and these dendrites are further periodically arranged with spatial period L. The tallest dendrites are located at $i=0$ and L, the next tallest one is located at $i=L/2$, and the shortest ones, all being the same size, are located at $i=L/4$ and $3L/4$. The heights of the four dendrites are denoted as y_1, y_2, and y_3, respectively. Figure 5(a) is a snapshot pattern of dendrites at $u_0=0.1$ and $L=120$. Figure 5(b) displays a semilogarithmic plot of the ratios of growth velocities $r_2=v_2/v_1$ and $r_3=v_3/v_2$ as a function of the height differences $\Delta y_2=y_1-y_2$

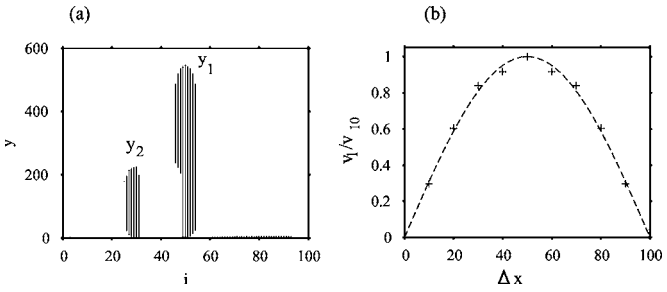

FIG. 4. (a) Snapshot growth pattern of two dendrites which grow from $i_2=30$ and $i_1=50$ for $u_0=0.1$ and $L=100$. (b) Ratio v_1/v_{10} of the growth velocity of the shorter dendrite, when the size difference Δy is equal to 150 for $u_0=0.1$ and $L=100$. The dashed curve is $\sin(\pi\Delta x/L)$.

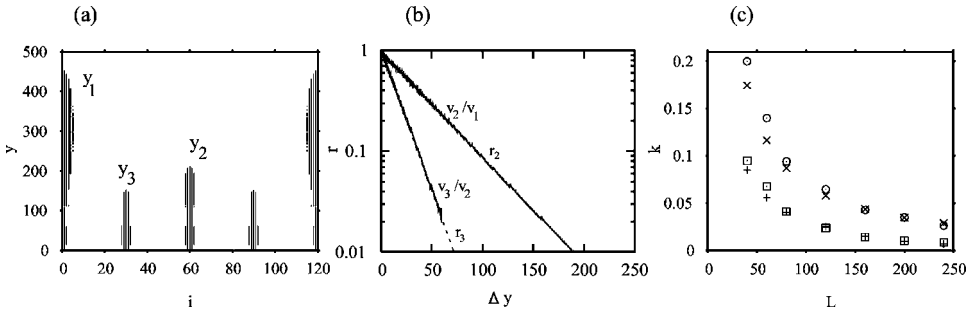

FIG. 5. (a) Snapshot growth pattern of two dendrites that grow from $i=0,30,60,90$ for $u_0=0.1$ and $L=120$. (b) The solid lines represent the ratios v_2/v_1 and v_3/v_2 as functions of the height differences $\Delta y_2=y_1-y_2$ and $\Delta y_3=y_2-y_3$. The dashed lines denote $r_2\sim\exp(-0.243\Delta y_2)$ and $r_3\sim\exp(-0.64\Delta y_3)$. The dashed lines (in particular the dashed line for r_2) are almost overlapped with the lines of v_2/v_1 and v_3/v_2, and the differences are indistinguishable in this plot. (c) Decay rates k_{12} and k_{13} of v_2/v_1 (square) and v_3/v_2 (circle) and $k_1(L)$ (plus) and $k_1(L/2)$ (cross)

and $\Delta y_3=y_2-y_3$. The ratios decay exponentially as $r_2\sim\exp(-k_{12}\Delta y_2)$ with $k_{12}\sim0.243$ and $r_3\sim\exp(-k_{13}\Delta y_3)$ with $k_{13}\sim0.64$. The ratio $r_1=v_3/v_1=r_2\times r_3$ does not exhibit a simple exponentail decay as a function of $\Delta y_1=y_1-y_3$, because r_1 is approximated by $\exp(-k_{12}\Delta y_2-k_{13}\Delta y_3)$, which is actually confirmed. Figure 5(c) displays decay rates k_{12} (square) and k_{13} (circle) as a function of L. Other marks represent $k_1(L)=1/2[-v/D+\sqrt{(v/D)^2+4(\pi/L)^2}]$ (plus) and $k_1(L/2)=1/2[-v/D+\sqrt{(v/D)^2+4\{\pi/(L/2)\}^2}]$ (cross). If all the dendrites grow with the same velocity v, the diffusion field satisfies Eq. (3). The boundary conditions are $u=0$ inside the dendrites. If all the dendrites are further assumed to be needles with zero thickness, the boundary conditions are $u=0$ on the lines $x=0, y<y_1$, $x=L/4, y<y_3$, $x=L/2, y<y_2$, and $x=3L/4, y<y_3$. The concentration field u can be expanded in a Fourier series as $u(x,y)=\Sigma_{n=1}^{N}a_n\sin\{(2n-1)\pi x/L\}e^{k_n(L)y}$ and it is approximated as $u(x,y)=a_{11}\sin(\pi x/L)e^{k_1(L)y}$ for $y_2<y<y_1$. Similarly, $u(x,y)=a_{12}\sin(2\pi x/L)e^{k_1(L/2)y}$ in the region $0<x<L/2$ and $y_3<y<y_2$, and $u(x,y)=a_{12}\sin[2\pi(x-L/2)/L]e^{k_1(L/2)y}$ in the region $L/2<x<L$ and $y_3<y<y_2$. The fairly good agreement between k_{12} and k_{13} with $k_1(L)$ and $k_1(L/2)$ implies that the ratios $r_2=v_2/v_1$ and $r_3=v_3/v_2$ can be approximated by $\exp[-k_1(L)\Delta y_2]$ and $\exp[-k_1(L/2)\Delta y_3]$. That is, the growth velocity of the shorter dendrites is proportional to the concentration field $u(x,y)$ at the tip position of the shorter dendrites, which is realized under the condition that the shorter dendrites do not exist.

V. SIMPLE NEEDLE MODEL FOR COMPETITIVE DYNAMICS AMONG DENDRITIC BRANCHES

On the basis of the numerical results elucidated in the previous section, we propose a simple needle model for competitive dynamics among dendritic branches. The thickness and the branching of each dendrite are neglected. We first explain the needle model for four dendrites at $i=0$, $L/4$, $2L/4$, $3L/4$, and L as shown in Fig. 5(a). For simplicity, we assume the mirror symmetry with respect to $y=L/2$. The tallest dendrites are located at $i=0$ and L, the next tallest one is located at $L/2$, and the third tallest at $L/4$ and $3L/4$, respectively. The heights of the dendrites are denoted as y_1, y_2, and y_3. The velocity of the tallest one is assumed to be constant v_1. The velocity v_2 of the second one is assumed to obey $v_2=v_1\exp[-k_1(L)(y_1-y_2)]$. The velocity v_3 of the third one is assumed to be $v_3=v_1\exp[-k_1(L)(y_1-y_2)]\times\exp[-k_1(L/2)(y_2-y_3)]=v_2\exp[-k_1(L/2)(y_2-y_3)]$. These relations can be generalized to a hierarchical structure of needles with the maximum rank number K as shown in Fig. 6(a) ($K=4$). The total number of needles in this hierarchical structure is $2^{K-1}+1$ and the tallest ones are located at $i=0$ and $i=2^{K-1}=L$. The jth ones are located at $(2m-1)\times2^{K-j}$, where $m=1,2,\ldots,2^{j-2}$. The velocity of the jth one is related to the velocity of the $(j-1)$th one as

$$v_j=v_{j-1}\exp\{-k_1(L/2^{j-2})(y_{j-1}-y_j)\}. \tag{9}$$

Here, we have neglected terms such as $\sin(\pi\Delta x/L)$ in Eq. (8) for the sake of simplicity. The relation of the growth velocities for dendrites is rewritten as a form of differential equation:

$$\frac{dy_j}{dt}=\frac{dy_{j-1}}{dt}\exp\{-k_1(L/2^{j-2})(y_{j-1}-y_j)\}. \tag{10}$$

This is our needle model for competitive dynamics among dendritic branches with a hierarchical structure. This equation can be explicitly solved as

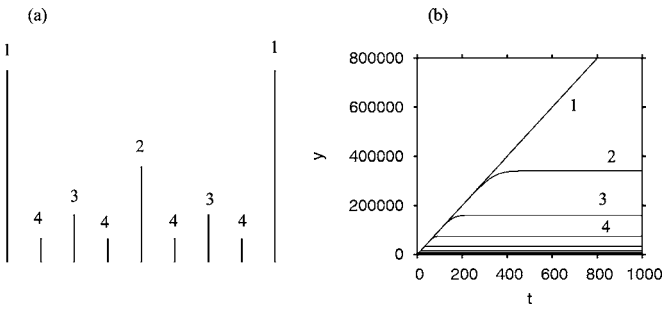

FIG. 6. (a) Configuration of a hierarchical structure with the maximum rank order $K=4$. (b) Time evolution of y_i for the needle model with $K=16$.

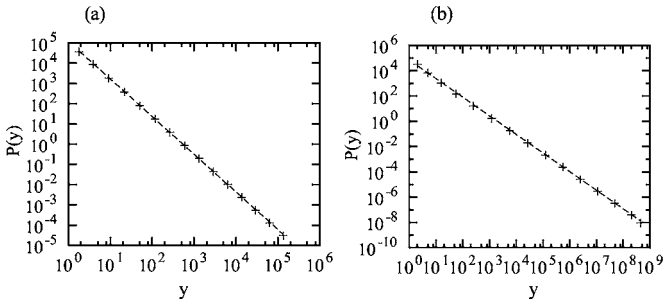

FIG. 7. (a) Height distribution $P(y)$ for $v=0.02$, $L=10^5$, and $k_1(L)=\pi/L$. (b) Height distribution $P(y)$ for $v=0.02$, $D=0.2$, and $k_1(L)=1/2[-v/D+\sqrt{(v/D)^2+4\{\pi/(L/2)\}^2}]$

$$\exp\{-k_1(L/2^{j-2})y_j(t)\}-\exp\{-k_1(L/2^{j-2})y_j(0)\}$$
$$=\exp\{-k_1(L/2^{j-2})y_{j-1}(t)\}-\exp\{-k_1(L/2^{j-2})y_{j-1}(0)\}.$$

Then, the height $y_j(t)$ at any time t is explicitly expressed as

$$y_j(t)=\frac{-1}{k_1(L/2^{j-2})}\ln[\exp\{-k_1(L/2^{j-2})y_j(0)\}-\exp\{-k_1(L/2^{j-2})y_{j-1}(0)\}+\exp\{-k_1(L/2^{j-2})y_{j-1}(t)\}], \quad (11)$$

where the tallest dendrite is assumed to grow at a constant velocity $y_1(t)=y_1(0)+vt$. Figure 6(b) displays the time evolution of $y_j(t)$ for a hierarchical structure with $K=16$ for $k_1(L)=\pi/L$, $L=10^5$, and $v=0.02$ by Eq. (11). The initial conditions are $y_j=(K+1-j)\ln 2$. The dendrites with the exception of the tallest one eventually stop growing. Figure 7(a) displays the height distribution $P(y)$ at the stationary state for the hierarchical structure with $K=16$ for $k_1(L)=\pi/L$, $L=10^5$, and $v=0.02$. The dashed line represents $P(y)\sim y^{1.86}$. If the argument in the logarithmic term in Eq. (11) is assumed to be a constant, $y_j\sim L/2^{j-2}$, and the number N_j of the jth dendrites is 2^{j-2}. Therefore, $N(y)=1/y$, and $P(y)\sim N(y)/(y/2)\sim 1/y^2$. The deviation of the exponent 1.86 from 2 might be due to the logarithmic term. Figure 7(b) displays the height distribution $P(y)$ for $k_1(L)=1/2[-v/D+\sqrt{(v/D)^2+4\{\pi/(L/2)\}^2}]$ for the same hierarchical structure with $K=16$ for $L=10^5$, $D=0.2$, and $v=0.02$. The height distribution is approximated by $P(y)\sim y^{-1.47}$. When L is sufficiently large, $k_1(L)$ is approximated as $k_1(L)\sim 2\pi^2/L^2$. If the logarithmic term in Eq. (11) is neglected, $y_j\sim L^2/2^{2j-4}$; therefore, $N(y)=1/y^{1/2}$ and $P(y)\sim y^{-1.5}$. The deviation of the exponent 1.47 from 1.5 is also due to the logarithmic term.

Our needle model can be generalized to a random system. Figure 8(a) displays an example of random dendritic branches. As shown in Fig. 8(a), we can assign a rank order to each dendritic branch. The order of the tallest branches is 1; they are located at $i=0$ and $i=L$. The order of the second one is 2, and it is located at i_2. The tallest ones between the first- and the second-order branches are expressed as order 3_1 and 3_2, which are located at i_{3_1} and i_{3_2}. Similarly, the tallest ones between the $(j-1)$th order and the $(j-1-k)$th branches $(1\leqslant k\leqslant j-2)$ are expressed as $j_1,j_2,\ldots$. The maximum number of the jth-order branches is 2^{j-2}, but it is generally smaller than the maximum number. The growth velocity of the jth-order branch is assumed to be determined by th e diffusion field, which is approximately given by an exponential function of the height difference. Thus, the growth velocity is expressed as $v_{j_l}(t)=v_1\exp\{-\Sigma_{m=1}^{j-1}k_1(L_{m_l})(y_{(m-1)_{l''}}-y_{m_{l'}})\}=v_{(j-1)_{l'}}\exp\{-k_1(L_{j_l})(y_{(j-1)_{l'}}-y_{j_l})\}$, where L_{j_l} is the spacing between two corresponding dendritic branches. The spacing L_{j_l} takes on a different value for each dendritic branch j_l in the jth rank order. For example, L_2 is the spacing between the two tallest branches and therefore $L_2=L$. Similarly, $L_{3_1}=i_2-0$, $L_{3_2}=L-i_2$, and $L_{4_1}=i_{3_1}-0$, $L_{4_2}=i_2-i_{3_1}$, $L_{5_1}=i_{4_3}-i_2$, $L_{6_1}=i_{4_3}-i_{5_1}$ and so on. These relations concerning the growth velocities are rewritten as coupled differential equations:

$$\frac{dy_{j_l}}{dt}=\frac{dy_{(j-1)_{l'}}}{dt}\exp\{-k_1(L_{j_l})(y_{(j-1)_{l'}}-y_{j_l})\}. \quad (12)$$

The growth velocity dy_{j_l}/dt of the jth-order branch cannot overcome the velocity $dy_{(j-1)_{l'}}/dt$ of the $(j-1)$th-order branch, because $\exp\{-k_1(L_{j_l})(y_{(j-1)_{l'}}-y_{j_l})\}<1$. Therefore, the rank order of dendritic branches does not change during

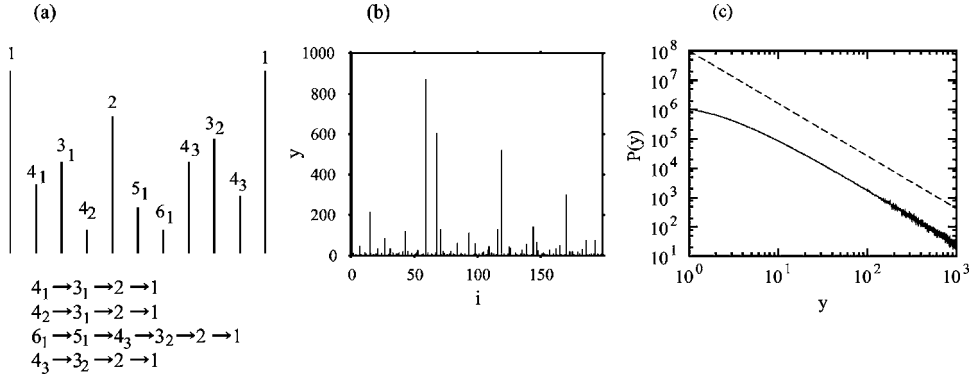

FIG. 8. (a) Random branches and their ordering. (b) Final pattern of y_j for $v=0.02$, $L=200$, and $k_1(L)=\pi/L$. (c) Height distribution $P(y)$ for $L=1000$, $v=0.02$, and $k(L)=\pi/L$. The dashed line denotes a power law $P\sim y^{-1.79}$.

the time evolution, and the spacing L_{j_l} also does not change in time. That is, the rank order and L_{j_l} are determined by the initial condition. This differential equation can also be explicitly solved as

$$y_{j_l}(t) = \frac{-1}{k_1(L_{j_l})} \ln[\exp\{-k_1(L_{j_l})y_{j_l}(0)\} - \exp\{-k_1(L_{j_l})y_{(j-1)_{l'}}(0)\} + \exp\{-k_1(L_{j_l})y_{(j-1)_{l'}}(t)\}]. \tag{13}$$

The height of each dendritic branch is completely determined by the initial conditions.

Figure 8(b) displays the final pattern of the dendritic branches, when the initial values of $y_i(0)$ are random numbers between 0 and 0.1 and $v=0.02$ and $L=200$. The decay rate $k(L)=\pi/L$ is used for the numerical simulation. A very large height difference appears among the dendritic branches, as a result of strong competition. Only two dendrites at $i=0$ and L grow at the constant velocity v. Figure 8(c) displays the height distribution $P(y)$ for $L=1000$, $v=0.02$, and $k(L)=\pi/L$. The dashed line denotes a power law with exponent 1.79. The exponent is roughly comparable to the exponent 1.86 for the hierarchical model and the exponent 1.9 for the coupled map lattice model in Fig. 1(c).

VI. SUMMARY

We have investigated the competitive dynamics among dendritic branches using a coupled map lattice. We have found an exponential decay law of the growth velocity for shorter dendrites. The height distribution exhibits a power law approximately. The decay rate of the growth velocity is related to the decay rate of the diffusion field. Then, we proposed a needle model for the competitive dynamics among dendritic branches on the basis of the interaction characterized by the exponential decay. The needle model can be solved explicitly, that is, the final distribution is completely determined by the initial conditions. The height distribution by the needle model is also approximated by a power law, and the exponent is roughly close to the value obtained by the coupled map lattice model. Our model is a very simple model but it could conceivably be an instructive one for general competitive systems.

Our results are qualitatively consistent with the results in [7,17], in that on exponential decay law of the growth velocity is found for shorter branches, and the screening effect is approximately expressed via $\tan\theta=(y_1-y_2)/(L/2)$ as shown in Fig. 3(a). We are now investigating experimentally the dendritic growth of NH_4Cl. We would like to compare the experimental results and the previous experimental results shown in [5,7] with our numerical results more quantitatively in the future.

[1] J. S. Langer, Rev. Mod. Phys. **52**, 1 (1980).
[2] *Dynamics of Curved Fronts*, edited by P. Pelce (Academic Press, San Diego, 1988).
[3] S. C. Huang and M. E. Glicksman, Acta Metall. **29**, 701 (1981).
[4] Q. Li and C. Beckermann, Phys. Rev. E **57**, 3176 (1998).
[5] Q. Li and C. Beckermann, Acta Mater. **47**, 2345 (1999).
[6] T. Honda, H. Honjo, and H. Katsuragi, J. Cryst. Growth **e225**, 5 (2005).
[7] Y. Couder, J. Maurer, R. González-Cinca, and A. Hernández-Machado, Phys. Rev. E **71**, 031602 (2005).
[8] G. Rossi, Phys. Rev. A **35**, 2246 (1987).
[9] Y. Huang, G. Ouillon, H. Saleur, and D. Sornette, Phys. Rev. E **55**, 6433 (1997).
[10] J. Krug, Adv. Phys. **46**, 139 (1997).
[11] T. Nagatani, J. Phys. A **24**, L449 (1991).
[12] H. Sakaguchi, Phys. Lett. A **313**, 188 (2003).
[13] R. Kobayashi, Physica D **63**, 410 (1993).
[14] A. Karma and W. J. Rappel, Phys. Rev. E **53**, R3017 (1996).
[15] H. Sakaguchi and S. Tokunaga, Prog. Theor. Phys. **110**, 1043 (2003).
[16] H. Sakaguchi and S. Tokunaga, Physica D **205**, 222 (2005).
[17] R. González-Cinca, Y. Couder, and A. Hernández-Machado, Phys. Rev. E **71**, 051601 (2005).
[18] H. Sakaguchi, J. Phys. Soc. Jpn. **67**, 96 (1998).
[19] H. Sakaguchi and M. Ohtaki, Physica A **272**, 300 (1999).
[20] H. Sakaguchi and M. Ohtaki, J. Phys. Soc. Jpn. **73**, 1723 (2004).
[21] H. Sakaguchi, T. Yoshida, S. Nakanishi, K. Fukami, and Y. Nakato, J. Phys. Soc. Jpn. **75**, 114002 (2006).